

Perturbative heavy quark-antiquark systems

M. Beneke

Theory Division, CERN, CH-1211 Geneva 23, Switzerland

E-mail: martin.beneke@cern.ch

ABSTRACT: In this review I cover recent developments concerning the construction of non-relativistic effective theories for perturbative heavy quark-antiquark systems and heavy quark mass definitions. I then discuss next-to-next-to-leading order results on quarkonium masses and decay, top quark pair production near threshold and QCD sum rules for Υ mesons. (November 1999, CERN-TH/99-355, hep-ph/9911490)

HEAVY QUARK effective field theory has profoundly influenced the way we think about mesons made of a heavy and a light quark [1]. It provides a systematic expansion in powers of α_s and Λ_{QCD}/m_Q . Perhaps more important, it separates hard (momenta $l \sim m_Q$) and soft ($l \sim \Lambda_{\text{QCD}}$) physics. Hard effects can be calculated; spin-flavour symmetry [2] relates soft effects and makes the framework predictive.

The construction of an effective theory for mesons made of a heavy quark and antiquark (“onia”) turned out to be more difficult. There are important differences between $Q\bar{Q}$ systems and $Q\bar{q}$ systems: the former develop weak-coupling bound states in the heavy quark limit, the latter don’t. The expansion parameter for onia is the velocity of the heavy quark, v , rather than Λ_{QCD}/m_Q . There is no flavour symmetry. But first of all, the presence of four momentum scales m_Q , $m_Q v$, $m_Q v^2$ and Λ_{QCD} rather than only two complicates the effective theory construction.

In a seminal paper Caswell and Lepage introduced effective field theory methods to QED bound state calculations [3]. The QCD equivalent, called non-relativistic QCD (NRQCD) [4], has now become an established tool in lattice simulations and for describing quarkonium production and decay [5]. However, for perturbative heavy quark-antiquark systems, by which I mean onia that satisfy $m_Q v^2 \gg \Lambda_{\text{QCD}}$ in addition to $v \ll 1$, NRQCD is not yet optimal. NRQCD factorizes the scale m_Q (and needs to assume only that $m_Q \gg \Lambda_{\text{QCD}}$), but does not deal with the

large scale hierarchy $m_Q v \gg m_Q v^2$. It does not make explicit the dominance of the static Coulomb force and the approximate quantum-mechanical nature of perturbative $Q\bar{Q}$ systems.

During the past two years progress on perturbative $Q\bar{Q}$ systems has been rapid. Some details remain to be clarified, but the effective field theory (EFT) picture is now essentially complete. Several advanced applications have been worked out. The use of effective theory may not be compulsory for perturbative $Q\bar{Q}$ systems. However, the gain in systematics in the expansion in v , transparency of language and, eventually, technical simplification, is enormous. In this sense effective field theory has had as profound an impact on understanding onia as it had on understanding heavy-light mesons.

1. Effective theories

1.1 NRQCD

Scattering processes at momentum transfer much smaller than m_Q are reproduced by the non-relativistic Lagrangian [4]

$$\begin{aligned} \mathcal{L}_{\text{NRQCD}} = & \psi^\dagger \left(iD^0 + \frac{\vec{D}^2}{2m_Q} \right) \psi + \frac{1}{8m_Q^3} \psi^\dagger \vec{D}^4 \psi \\ & - \frac{d_1 g_s}{2m_Q} \psi^\dagger \vec{\sigma} \cdot \vec{B} \psi + \frac{d_2 g_s}{8m_Q^2} \psi^\dagger \left(\vec{D} \cdot \vec{E} - \vec{E} \cdot \vec{D} \right) \psi \\ & + \frac{d_3 i g_s}{8m_Q^2} \psi^\dagger \vec{\sigma} \cdot \left(\vec{D} \times \vec{E} - \vec{E} \times \vec{D} \right) \psi + \dots \\ & + \text{antiquark terms} \end{aligned}$$

$$+ \sum_{\Gamma} \frac{d_{\Gamma}}{m_Q^2} (\psi^{\dagger} \Gamma \chi) (\chi^{\dagger} \Gamma \psi) + \dots + \mathcal{L}_{\text{light}}. \quad (1.1)$$

Loop graphs involve large momentum of order m_Q . The large momentum regions are accounted for by adapting the couplings $d_i(\Lambda)$ order by order in $\alpha_s(m_b)$. By adding more operators the full scattering amplitude can be reproduced to any accuracy in an expansion in α_s and v .

The Lagrangian (1.1) appears similar to the heavy quark effective Lagrangian, except that it contains an antiquark clone of the single heavy quark sector and a quark-antiquark sector (operators made out of ψ and χ), which is absent in HQET. Indeed, the couplings in the single quark (antiquark) sector are identical in HQET and NRQCD to all orders in α_s [6], if the same factorization prescription is used. However, the power counting is generally different. For example, the kinetic energy term $\vec{\partial}^2/(2m_Q)$ is expected to be of the same order as $i\partial_0$, because non-relativistic $Q\bar{Q}$ systems have momenta of order $m_Q v$ and energies of order $m_Q v^2$. The situation is actually more complicated. Because the kinetic term is part of the leading order Lagrangian, scattering amplitudes computed with NRQCD depend on m_Q , v and the cut-off Λ in a non-trivial way. If one chooses Λ several times $m_Q v$, every Feynman diagram is a complicated function of v . This should be compared to HQET, where, choosing the cut-off several times Λ_{QCD} , every Feynman integral is just a number. The dependence on m_Q is fixed by the over-all power and coupling of the operator in the effective Lagrangian. There is no problem of principle with non-trivial dependence on v , if the Lagrangian is defined with a hard cut-off larger than $m_Q v$ and if the NRQCD quantities are computed non-perturbatively as in lattice NRQCD.

However, for perturbative calculations of perturbative $Q\bar{Q}$ systems this is inconvenient. First, one calculates too much, because one will need the NRQCD amplitude only to some accuracy in the v expansion. The full v dependence has a technical price. It is more difficult to compute an integral which is a function of v than an integral which is just a number. Second, one would like to use dimensional regularization (DR). Here the subtleties arise, because DR gets NRQCD in-

tegrals, written down naively, wrong. Because the integrand depends on m_Q , the dependence on the scale μ of DR corresponds to a cut-off $\Lambda \gg m_Q$ instead of $m_Q \gg \Lambda \gg m_Q v$ [7]. Consequently, QCD is not matched correctly onto NRQCD. This difficulty is related to the existence of two scales, $m_Q v$ and $m_Q v^2$ in NRQCD. The first attempt to separate these scales was made in [8] in the context of cut-off regularizations and time-ordered perturbation theory in Coulomb gauge. This work introduced the important distinction of soft and ultrasoft gluons (photons) and the multipole expansion for ultrasoft gluons, but the construction remained complicated and somewhat qualitative. Subsequent work [9, 10, 11] identified different momentum regions that should contribute to NRQCD integrals, but dropped the soft region identified in [8]. These early works introduced many of the important concepts that appear in a non-relativistic EFT construction, pointed towards the necessity to perform expansions of Feynman *integrand*s [6, 7, 10] in order to define NRQCD in DR, but did not yet provide a complete solution to the problem of separating the scales $m_Q v$ and $m_Q v^2$ and of defining NRQCD in DR.

1.2 Threshold expansion

Take an on-shell scattering amplitude of heavy quarks with momentum $m_Q v$ and gluons with momentum $m_Q v^2$ in QCD. The basic problem is to construct *term by term* the expansion of this amplitude in v . Such a construction may introduce divergent loop integrals in intermediate steps, even if the original expression was finite. We would like to use DR to regularize these divergences and we require that any integral that we have to compute contributes only to a single order in the v expansion. Solving this problem is equivalent to constructing a non-relativistic effective theory in DR with easy velocity power counting and all scales separated.

The expansion method described in [12] begins by identifying the relevant momentum regions in loop integrals, which follow from the singularity structure of the Feynman integrand. This is analogous to identifying hard, collinear and soft particles in high-energy scattering of massless particles. For non-relativistic scatter-

ing of heavy quarks, one finds four momentum regions:

$$\begin{aligned}
\text{hard (h): } & l_0 \sim \vec{l} \sim m_Q, \\
\text{soft (s): } & l_0 \sim \vec{l} \sim m_Q v, \\
\text{potential (p): } & l_0 \sim m_Q v^2, \vec{l} \sim m_Q v, \\
\text{ultrasoft (us): } & l_0 \sim \vec{l} \sim m_Q v^2.
\end{aligned} \tag{1.2}$$

Both, heavy quarks and gluons can be hard, soft and potential, but only gluons can be ultrasoft. (In the following, ‘‘gluons’’ may include all other massless modes, i.e. light quarks and ghosts.)

The threshold expansion is constructed by writing a Feynman diagram in QCD as a sum of terms that follow from dividing each loop momentum integral into these four regions. The division is done implicitly, through expansion of the propagators. No explicit cut-offs are needed. The expansion rule is that in every region one performs a Taylor expansion in the quantities which are small in that region. An immediate consequence of this is that every integral contributes only to a single power in the velocity expansion.

To give an example of the expansion rules, consider the propagator of a heavy quark with momentum $(q/2 + l_0, \vec{p} + \vec{l})$,

$$\frac{1}{l_0^2 - \vec{l}^2 - 2\vec{p} \cdot \vec{l} - \vec{p}^2 + ql_0 + y + i\epsilon}, \tag{1.3}$$

and assume that \vec{p} scales as mv and $y = q^2/4 - m^2$ as mv^2 . When l is hard, we expand the terms involving \vec{p} and y and the leading term in the expansion scales as v^0 . When l is soft, the term ql_0 is largest and the remaining ones are expanded. The propagator becomes static and scales as v^{-1} . Notice that this means that the kinetic energy term in the NRQCD Lagrangian is treated as an interaction term in the soft region, because it is small. When l is potential, the propagator takes its standard non-relativistic form after expansion of l_0^2 and scales as v^{-2} . The gluon propagator takes its usual form, when the gluon line is soft and ultrasoft and scales as v^{-2} and v^{-4} , respectively. If the gluon momentum is potential, one can expand l_0^2 and the interaction becomes instantaneous. If we add the scaling rules for the loop integration measure,

$d^4l \sim 1$ (h), v^4 (s), v^5 (p), v^8 (us), we can immediately estimate the size of the leading term from a given region. It is clear that these rules can be reformulated as an effective Lagrangian. The hard subgraphs give the dimensionally regularized couplings in the NRQCD Lagrangian. On the other hand, the distinction of soft, potential and ultrasoft momentum implies a manipulation of the NRQCD Lagrangian that is not evident from (1.1).

It is instructive to discuss the physical interpretation of the terms that arise in the threshold expansion on a particular diagram. Take the planar, 2-loop correction to the electromagnetic heavy quark production vertex [12], i.e. the matrix element $\langle \bar{Q}(p_1) \bar{Q}(p_2) | \bar{Q} \gamma^\mu Q | 0 \rangle$. Many of the possible combinations of h, s, p and us loop momentum result in scaleless integrals, which are zero in dimensional regularization. Such scaleless integrals gain significance only in the context of the renormalization group, in which case one has to be more careful about the nature of $1/\epsilon$ poles. The non-vanishing configurations are shown in figure 1. Every diagram stands for a series in v that arises from the expansion of the integrand in a particular loop momentum configuration, but every integral in this series contributes only to a single power of v .

The h-h configuration is a 2-loop correction to the coefficient functions in the non-relativistic expansion of the current $\bar{Q} \gamma^i Q \rightarrow C_1 \psi^\dagger \sigma^i \chi + \dots$. The leading term is of order $\alpha_s^2 v^0$. There are two possibilities for having 1-loop hard subgraphs. The first one (upper right) represents a 1-loop renormalization of the non-relativistic external current followed by exchange of a potential gluon. At leading order in the v expansion potential gluon exchange can be interpreted as an interaction through the Coulomb potential $-\alpha_s C_F/r$. This contribution is of order α_s^2/v . The second h-p term corresponds to the insertion of a four-fermion operator $(\psi^\dagger \kappa \psi)(\chi^\dagger \kappa \chi)$ from the NRQCD Lagrangian. This contribution begins at order $\alpha_s^2 v$. The soft subgraph in the s-p term can be interpreted as an instantaneous interaction, because a soft subgraph can be expanded in the zero components of its external momenta. The s-p graph corresponds to an insertion of (part of) the 1-loop corrected Coulomb

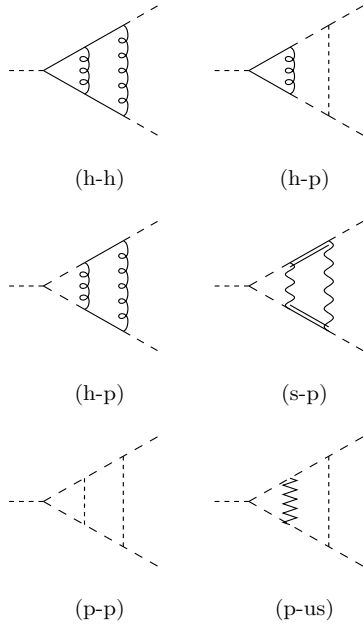


Figure 1: Decomposition of the planar, 2-loop vertex integral in the threshold expansion. Line coding: solid and curled – hard quarks and gluons, respectively; double line and wavy – soft quarks and gluons; long- and short-dashed – potential quarks and gluons; zigzag – ultrasoft gluons.

potential plus higher potentials more singular in r . It contributes at order α_s^2/v . The p-p term is dominant at small v . The double insertion of the Coulomb potential contributes at order α_s^2/v^2 . If v is counted as α_s , as forced upon us by the dynamics of perturbative, non-relativistic bound states, this term is unsuppressed relative to the tree graph. This shows the need to partially sum the expansion in α_s to all orders. Finally, ultrasoft gluon exchange is of order α_s^2/v . This is actually an over-estimate. After combining all diagrams with an ultrasoft gluon, one finds that the coupling of ultrasoft gluons to heavy quarks has at least a factor of v . This cancellation is manifest in Coulomb gauge, in which only the spatial component of the gauge field can be ultrasoft. Hence the p-us term is of order $\alpha_s^2 v$. Note that in an expansion scheme in which $v \sim \alpha_s$, only four of the six terms in figure 1 are needed at next-to-next-to-leading (NNLO) order.

1.3 Effective theory again: PNRQCD

We have now defined NRQCD and can compute

its couplings in DR. This leads to a new set of graphs in which hard subgraphs have been contracted to a point. The remaining loop integrals can still be soft, potential or ultrasoft. One could introduce different fields for p, s and us quarks and gluons and implement the threshold expansion rules at the level of effective propagators and vertices [13]. But since soft heavy quarks and gluons and potential gluons do not appear as external lines for non-relativistic systems, we can integrate them out. As can be seen from the structure of the threshold expansion, soft subgraphs have the same combinatorial structure as hard subgraphs. They can be contracted to effective operators, which are non-local in space, but local in time (instantaneous). These effective operators provide a generalized notion of the heavy quark potential. The resulting effective theory contains only potential quarks and ultrasoft gluons. Velocity power counting is then trivial. The scheme is as follows:

$$\begin{aligned}
 \mathcal{L}_{\text{QCD}} [Q(h, s, p), g(h, s, p, us)] & \quad \mu > m \\
 \downarrow \\
 \mathcal{L}_{\text{NRQCD}} [Q(s, p), g(s, p, us)] & \quad mv < \mu < m \\
 \downarrow \\
 \mathcal{L}_{\text{PNRQCD}} [Q(p), g(us)] & \quad \mu < mv
 \end{aligned}$$

Such a construction has been proposed first, by tree level matching, in [14]. I follow [14] in calling the second EFT potential NRQCD (PNRQCD). In the context of the threshold expansion, which provides a matching prescription for loop graphs, PNRQCD has been discussed in [15, 16]. A somewhat different, but probably conceptually equivalent construction has been proposed recently in [17].

In general the PNRQCD Lagrangian can be written as

$$\mathcal{L}_{\text{PNRQCD}} = \mathcal{L}'_{\text{NRQCD}} + \mathcal{L}_{\text{non-local}}. \quad (1.4)$$

$\mathcal{L}_{\text{non-local}}$ collects all non-local interactions. The local interactions are exactly those of NRQCD, but the interpretation is different, because only potential heavy quarks and ultrasoft gluons are left over. In diagrams constructed from $\mathcal{L}'_{\text{NRQCD}}$ the gluon propagators are always expanded according to their ultrasoft scaling rule and the

heavy quark propagator has the familiar non-relativistic form, while in diagrams constructed from $\mathcal{L}_{\text{NRQCD}}$ gluons are also soft and potential and the heavy quark propagator can also be static. Because only potential quarks and ultrasoft gluons are left in PNRQCD, the interaction terms have definite velocity scaling rules. A potential quark propagator in coordinate space scales as v^3 , so a quark field in PNRQCD scales as $v^{3/2}$. An ultrasoft gluon field counts v^2 .

Integrating out potential gluon exchange between a quark and an antiquark at tree level gives the leading order Coulomb potential. The unperturbed PNRQCD Lagrangian is

$$\begin{aligned} \mathcal{L}_{\text{PNRQCD}}^0 = & \quad (1.5) \\ & \psi^\dagger \left(i\partial^0 + \frac{\vec{\partial}^2}{2m_Q} \right) \psi + \chi^\dagger \left(i\partial^0 - \frac{\vec{\partial}^2}{2m_Q} \right) \chi \\ & + \int d^3\vec{r} [\psi^\dagger T^A \psi](\vec{r}) \left(-\frac{\alpha_s}{r} \right) [\chi^\dagger T^A \chi](0). \end{aligned}$$

Since $v \sim \alpha_s(m_Q v)$ is assumed, all terms scale as v^5 ; the Coulomb interaction cannot be treated as a perturbation as is of course anticipated. One can rewrite the PNRQCD Lagrangian in terms of a ‘tensor field’ $[\psi \otimes \chi^\dagger](t, \vec{R}, \vec{r})$ that depends on the cms and relative coordinates. The unperturbed Lagrangian describes free propagation (with mass $2m$) in the cms coordinate. The propagation of $[\psi \otimes \chi^\dagger](t, \vec{R}, \vec{r})$ in its relative coordinate is given by the Coulomb Green function of a particle with reduced mass $m/2$. In calculating diagrams with Coulomb Green functions, one sums corrections of order $(\alpha_s/v)^n$ to all orders. The remaining terms can be treated as perturbations in v and α_s around the unperturbed Lagrangian.

Higher order non-local interactions follow after matching potential gluon exchange to better accuracy and after integrating out soft loops. We can match assuming $\alpha_s \ll v$, and treat the Coulomb potential as a perturbation when matching NRQCD on PNRQCD. A general non-local operator is a function of r and derivatives ∂_i acting on the (anti)quark field. It is non-polynomial in r , but polynomial in ∂_i . In general, it may have ultrasoft gluon fields attached to it. Non-local operators are singular, for example $\alpha_s \delta^{(3)}(\vec{r})$ or α_s^2/r^2 . These singularities are harmless, be-

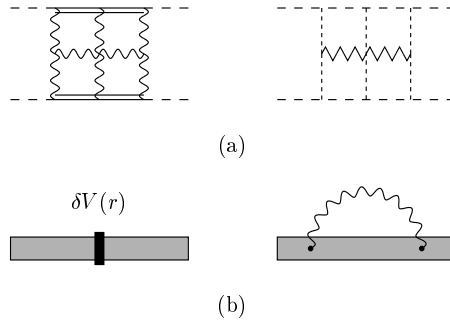


Figure 2: (a) s-s region that gives rise to an infrared logarithm (left); p-p-us region which contains the corresponding ultraviolet logarithm. (b) In PNRQCD notation the two NRQCD graphs in (a) are interpreted as a (Coulomb) potential insertion (left) and an ultrasoft 1-loop diagram (right). The shaded bar represents the propagation of the $Q\bar{Q}$ according to the Coulomb Green function. Line coding as in figure 1.

cause PNRQCD is defined with a cut-off (we imply dimensional regularization) and more singular non-local operators are in fact suppressed in v . The dimensionally regulated quark-antiquark potential up to order v^7 , projected on a colour singlet, spin-1 $Q\bar{Q}$ pair can be found in [16].

Potentials are short-distance coefficients, i.e. they are for PNRQCD what the d_i in (1.1) are for NRQCD. Consider the Coulomb potential in (1.5). Its coefficient is renormalized such that

$$\alpha_s \rightarrow \alpha_s(\mu) v_c(\alpha_s, \mu r). \quad (1.6)$$

The coefficient function $v_c(\alpha_s, \mu r)$ contains logarithms of μr , which are analogous to logarithms of the heavy quark mass in the coefficient functions of the NRQCD Lagrangian. Up to order α_s^2 , to which $v_c(\alpha_s, \mu r)$ is known exactly [18], all logarithms $\ln \mu r$ can be absorbed into $\alpha_s(1/r)$. This is no longer true at three loops. There exists an uncancelled infrared divergence in the left diagram of figure 2a [19] which, after subtraction of the pole in DR, gives rise to a logarithm not related to the running coupling. This logarithm is analogous to a non-vanishing anomalous dimension of local operators in the NRQCD Lagrangian. The scale dependence is cancelled for a physical process by the scale dependent PNRQCD matrix element, in this particular case the right diagram of figure 2a. In PNRQCD

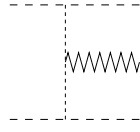


Figure 3: NRQCD graph that generates the mixed non-local/ultrasoft interaction in (1.8). Line coding as in figure 1.

notation, which does not make use of potential and soft lines, the correspondence is shown in figure 2b. The interpretation of potentials as matching coefficients implies that the Coulomb potential is not identical to the static potential defined as the vacuum expectation of a Wilson loop in the limit $T \rightarrow \infty$ [20]. The Coulomb potential is logarithmically sensitive to the ultrasoft scale, but it is not infrared divergent. This statement applies to any other potential.

Although the local interactions in (1.4) are the same as those in NRQCD, we must write them in a different form to account for the expansion rules for ultrasoft gluons. When an ultrasoft gluon line with momentum l connects to a quark line with momentum $k - l/2$ for the incoming and $k + l/2$ for the outgoing quark line, the threshold expansion instructs us to expand the quark-gluon vertex and quark propagator in $\vec{l}/\vec{k} \sim v$. All gluon interaction terms in $\mathcal{L}'_{\text{NRQCD}}$ should be understood as multipole-expanded, for instance [8, 10]

$$[\psi^\dagger A^i \partial^i \psi](x) \equiv \psi^\dagger(x) A^i(t, 0) \partial^i \psi(x) + \psi^\dagger(x) (x^j \partial^j A^i(t, 0)) \partial^i \psi(x) + \dots, \quad (1.7)$$

and likewise for all other terms in the NRQCD Lagrangian. The leading ultrasoft interactions follow from multipole expansion of the gauge field terms in $\psi^\dagger (iD^0 + \vec{D}^2 / (2m_Q)) \psi$ in (1.1) together with a non-abelian non-local term that comes from matching the graph in figure 3 on PNRQCD. The following collects all ultrasoft interactions up to order $v^{13/2}$:

$$\begin{aligned} \mathcal{L}_{us} = & g_s [\psi^\dagger T^A \psi](x) A^{0A}(t, 0) \\ & + g_s [\psi^\dagger T^A \psi](x) x^i \partial^i A^{0A}(t, 0) \\ & - \frac{ig_s}{2m_Q} [\psi^\dagger (\overleftarrow{\partial}^i - \overrightarrow{\partial}^i) T^A \psi](x) A^{iA}(t, 0) \\ & + \text{antiquark terms} \end{aligned}$$

$$\begin{aligned} & - \int d^3 \vec{r} [\psi^\dagger T^B \psi](x + \vec{r}) [\chi^\dagger T^C \chi](x) \\ & \cdot \left(-\frac{\alpha_s}{r} \right) g_s f^{ABC} r^i A^{iA}(t, 0) \end{aligned} \quad (1.8)$$

The first line scales as $v^{1/2}$ relative to the leading order v^5 terms in the PNRQCD Lagrangian. The other three interaction terms scale as $v^{3/2}$. Using $[x^i, \vec{\partial}^2] = -2\partial^i$ and the equation of motion at leading order in v , which includes the Coulomb potential, the $v^{3/2}$ interactions combine into a chromo-electric dipole operator up to higher order terms. (Note that this shows that the distinction of non-local and local operators in PNRQCD is ambiguous, because they can be converted into each other by the equation of motion. Likewise a classification in powers of $1/m_Q$ is not useful.) Introducing the ultrasoft covariant derivative $D^0 = \partial^0 - ig_s A^0(t, 0)$, we obtain

$$\mathcal{L}_{\text{PNRQCD}} = \quad (1.9)$$

$$\begin{aligned} & \psi^\dagger(x) \left(iD^0 + \frac{\vec{\partial}^2}{2m_Q} - g_s x^i E^i(t, 0) \right) \psi(x) \\ & + \text{antiquark terms} \\ & + \int d^3 \vec{r} [\psi_a^\dagger \psi_b](x + \vec{r}) V_{ab;cd}(r, \partial^i) [\chi_c^\dagger \chi_d](x) \end{aligned}$$

where

$$V_{ab;cd}(r, \partial^i) = T_{ab}^A T_{cd}^A \cdot \left(-\frac{\alpha_s}{r} \right) + \delta V_{ab;cd}(r, \partial^i) \quad (1.10)$$

This Lagrangian is manifestly invariant under ultrasoft gauge transformations $U(t, 0)$. Note that the spatial components of the gauge field transform covariantly under ultrasoft gauge transformations. Beyond tree-level the coefficient of the chromo-electric dipole operator receives corrections that can be computed in an expansion in α_s . The PNRQCD Lagrangian (1.9) appears to be equivalent to the Lagrangian derived in [14]. The difference is that [14] introduces a colour decomposition of the tensor field $[\psi \otimes \chi^\dagger](t, \vec{R}, \vec{r})$ and expresses the Lagrangian in terms of a colour singlet and a colour octet field S and O .

A Green function with no external ultrasoft lines requires at least two ultrasoft interactions. The leading ultrasoft correction is order v from the ultrasoft covariant derivative in (1.9). However, we can use an ultrasoft gauge transformation to gauge A^0 away, and hence the leading

ultrasoft correction is order v^3 . The Lagrangian (1.9) can be used to compute all leading ultrasoft contributions. In particular, ultraviolet renormalization of ultrasoft graphs cancels the scale dependence of the potentials to order v^3 . In [21] the scale dependence of the potentials has been computed using this correspondence.

1.4 Non-relativistic renormalization group

The scale hierarchy $m_Q \gg m_Q v \gg m_Q v^2$ also implies large logarithmic corrections $\alpha_s \ln v$ and $\alpha_s \ln v^2$ to the coefficient functions. These logarithms can be summed to all orders in perturbation theory as follows:

- 1) Match QCD and NRQCD at a scale $\mu_h \sim m_Q$, i.e. compute the coefficients d_i as expansions in $\alpha_s(\mu_h)$.
- 2) Compute the renormalization group scaling of the d_i in NRQCD and evolve them to a scale $\mu_s \sim m_Q v \sim 1/r$.
- 3) Match NRQCD and PNRQCD at the scale μ_s , i.e. compute the potential coefficients v_i as expansions in $\alpha_s(\mu_s)$ and in terms of the $d_i(\mu_s)$.
- 4) Compute the renormalization group scaling of the potentials in PNRQCD and evolve them to a scale $\mu_{us} \sim m_Q v^2 \sim m_Q \alpha_s^2$.
- 5) Compute the PNRQCD matrix elements with ultraviolet subtraction scale μ_{us} .

I briefly discuss items 2) and 4), but note that an explicit calculation remains yet to be done.

NRQCD contains a single-heavy quark sector, which is identical to heavy quark effective theory (HQET). Since heavy quark-antiquark operators do not mix into this sector, its renormalization can be discussed separately. Operator renormalization in NRQCD arises from ultraviolet divergences in potential and soft loops. The single-heavy quark sector has no potential loops (all quark poles on one side of the real axis in the complex plane of loop momentum zero components); the anomalous dimension matrices are identical to those in HQET. It is convenient not to introduce non-local time-ordered product operators as is usually done in HQET, but to have

lower dimensional operators mix into higher dimensional ones. For example, a vertex diagram with two insertions of the chromo-magnetic operator of (1.1) requires a counterterm proportional to the Darwin interaction, hence

$$\mu_1 \frac{d}{d\mu_1} d_2 = -\frac{5\alpha_s}{2\pi} d_1^2 + \dots \quad (1.11)$$

etc.. The single-heavy quark sector mixes into heavy quark-antiquark operators. These operators are renormalized by soft and potential loops. Mixing through potential loops is responsible for the scale dependence of the quark-antiquark current $\psi^\dagger \sigma^i \chi$ that appears first at two loops [22, 23]. Higher dimension operators in the single-heavy quark sector can mix into lower dimension operators in the heavy quark-antiquark sector through potential loops, because potential gluon exchange can contribute factors $m_Q/|\vec{p}|$, where \vec{p} is a relative momentum of order $m_Q v$. This never happens for soft loops. One can introduce two separate renormalization scales μ_1 and μ_2 for soft and potential loops and compute the corresponding anomalous dimension matrices. NRQCD coefficient functions $C_i(\mu_1, \mu_2)$ then depend on both scales. In the end we only need $C_i(\mu, \mu)$, which evolves with the sum of the two anomalous dimension matrices and the distinction is not necessary. However, the fact that potential loops are infrared finite tells us that the evolution in μ_2 stops at a scale of order $m_Q v$. Soft loops are not always infrared finite; this connects the evolution in μ_1 to the ultrasoft region.

Identifying $\mu_1 = \mu_2$ the NRQCD evolution terminates at the scale μ_s at which one matches to PNRQCD. The evolution of the potentials and other operators such as the chromo-electric dipole operator is then determined by the ultraviolet behaviour of ultrasoft loops.

A different implementation of renormalization group scaling from the one presented here has been suggested in [17]. In this case, too, an explicit calculation of operator renormalization has not yet been performed and the equivalence of the two approaches remains to be demonstrated.

1.5 $\Lambda_{\text{QCD}} \sim m_Q v^2$ or larger

The theoretical framework described so far re-

quires $m_Q v^2 \gg \Lambda_{\text{QCD}}$. Nice as it may be, it can be applied safely only to extremely elusive systems such as toponium. There will be non-perturbative corrections suppressed by powers of $\Lambda_{\text{QCD}}/(m_Q v^2)$ in addition to what I discussed above, which can be estimated by applying an operator product expansion to PNRQCD matrix elements [24]. In case of toponium these corrections are estimated to be small for the inclusive production cross section. Note that there are no non-perturbative modifications of the potentials, because they are short-distance objects.

What happens if $m_Q v^2$ is not that large?

If $m_Q \gg \Lambda_{\text{QCD}} \gtrsim m_Q v$, PNRQCD makes no sense. One can use NRQCD, but the NRQCD matrix elements are non-perturbative.

If $m_Q v \gg \Lambda_{\text{QCD}} \gtrsim m_Q v^2$, one can match perturbatively (in $\alpha_s(m_Q v)$) to PNRQCD, but since $\alpha_s(mv^2) \sim 1$ the self-coupling of ultrasoft gluons is unsuppressed. Velocity power counting is different from the one above which used $\alpha_s(mv^2) \sim \alpha_s(m_Q v) \sim v$. Non-perturbative gluons screen the ultrasoft scale $m_Q v^2$ and Λ_{QCD} takes its role. The coupling of ultrasoft gluons to heavy quarks is non-perturbative but small, of order $\Lambda_{\text{QCD}}/(m_Q v)$. Hence ultrasoft effects enter a heavy quark-antiquark scattering amplitude as an uncalculable non-perturbative contribution beginning at order $(\Lambda_{\text{QCD}}/(m_Q v))^2$. Up to this accuracy the amplitude is still determined by potentials. In particular, the potentials and the scale dependence of PNRQCD matrix elements remain perturbatively calculable.

2. Heavy quark mass definitions

Before turning to applications of non-relativistic field theory, I discuss the concept of the heavy quark mass. The (P)NRQCD Lagrangian is normally expressed in terms of the quark pole mass and this has been assumed so far. If not I should have added a term $\delta m_Q \psi^\dagger \psi$ to the (P)NRQCD Lagrangian. There are good reasons to make use of this option, related to the fact that the pole mass, though an infrared safe quantity in perturbation theory [25], incorporates uncalculable long-distance contributions of order Λ_{QCD} . Originally discovered and discussed in the context of HQET [26, 27, 28], the problem is acute when-

ever heavy quarks are not off-shell by an amount of order m_Q^2 . Recently there has been renewed interest in this problem in the context of $Q\bar{Q}$ systems [29, 30] and suitable alternative definitions of the heavy mass have been proposed and used in applications. Such masses have the generic property that they differ from the pole mass by an amount linear in a subtraction scale μ_f [28]. In this section I review the currently used mass definitions.

2.1 $\overline{\text{MS}}$ and pole mass

The $\overline{\text{MS}}$ mass $\overline{m}_Q(\mu)$ is the coefficient of the operator $\bar{Q}Q$ in QCD subtracted in the $\overline{\text{MS}}$ scheme. It is best understood as a coupling constant just as α_s . The $\overline{\text{MS}}$ mass is scale-dependent. The scale dependence is related to loop momenta $l \gg m_Q$. For this reason, it makes no sense to evolve the $\overline{\text{MS}}$ mass to scales parametrically smaller than m_Q . While formally possible, this generates fake logarithms of the ratio of scales. However, $\overline{m}_Q \equiv \overline{m}_Q(\overline{m}_Q)$ is a very useful reference parameter, just as $\alpha_s(m_Z)$.

The pole mass is the location of the pole in the full heavy quark propagator. (The weak interactions are switched off, so that quarks are stable. A finite decay width would not alter the conclusion of this subsection [31].) As such it is defined order by order in perturbation theory. Its relation to the $\overline{\text{MS}}$ mass is given by

$$\frac{m_Q}{\overline{m}_Q} = 1 + \sum_{n=1} k_n \alpha_s(\overline{m}_Q)^n. \quad (2.1)$$

For b quarks, neglecting internal the charm quark mass effects,

$$\begin{aligned} k_1 &= 0.424, & k_2 &= 0.940, \\ k_3 &= 3.096, & k_4 &= 13.60 \end{aligned} \quad (2.2)$$

The first two coefficients are known analytically [32], the third is known numerically [33]. For the fourth order coefficient I have used the so-called “large- β_0 ” estimate [34], which turned out to approximate $k_{2,3}$ very well.

Neither of the two masses is a useful parameter for perturbative calculations of $Q\bar{Q}$ systems. The $\overline{\text{MS}}$ mass would imply $\delta m_Q \sim m_Q \alpha_s$ and hence $\delta m_Q \psi^\dagger \psi \sim v^4$ would dominate the (P)NRQCD Lagrangian. One must have $\delta m_Q \sim$

$m_Q v^2$ or smaller. The pole mass is long-distance sensitive at order Λ_{QCD} . There would be nothing wrong with this if not for the following two facts: first, the quantities we would like to compute with non-relativistic field theory such as correlation functions of two heavy quark currents near threshold are less long-distance sensitive than the pole mass. This desirable property is lost, if one uses renormalization conventions which are more long-distance sensitive than the quantity of interest. Second, long-distance sensitivity is related to large perturbative corrections through infrared renormalons [35]. Here this means that series expansions diverge as $(2\beta_0)^n n! n^b$, where β_0 is defined through $d\alpha_s/d\ln\mu^2 = -\beta_0\alpha_s^2 + \dots$. The divergence enters less long-distance sensitive quantities only through $k_{n+1} \sim (2\beta_0)^n n! n^b$ and would be much milder, if a suitable mass renormalization convention were implied. For the following discussion it is useful to introduce an ‘‘asymptotic counting’’ for perturbative coefficients. The asymptotic counting of the coefficients (2.2) is $k_n \sim (n-1)! \mu/\bar{m}_Q$, where the definition of k_n has been generalized to an expansion in $\alpha_s(\mu)$ and we neglect the factors $(2\beta_0)^n$ and n^b in this schematic notation. I will also call a series expansion ‘‘convergent’’, if it diverges less rapidly than the k_n . Coefficients of ‘‘convergent’’ series count as order 1 and terms in a convergent series are counted only according to their power in α_s .

Asymptotic counting may appear abstract and irrelevant to next-to-next-to-leading order calculations. The physical systems which we discuss later (and numerous quantities related to B meson decays) show that this is not so. This has led to heavy quark mass definitions, which satisfy $\delta m_Q \sim m_Q v^2$ and are convergent in asymptotic counting.

2.2 PS mass

The potential subtraction (PS) scheme [29] is based on the observation that there is a cancellation of divergent series behaviour in the combination $2m_Q + [V(r)]_{\text{Coulomb}}$. This can be seen explicitly at 1-loop and in the large- β_0 approximation [29, 30] by combining the results of [34, 36] and by a diagrammatic argument at two loops [29] and, probably, in higher orders. The potential subtracted (PS) mass at subtraction scale μ_f

is defined by

$$m_{Q,\text{PS}}(\mu_f) = m_Q + \frac{1}{2} \int_{|\vec{q}| < \mu_f} \frac{d^3\vec{q}}{(2\pi)^3} [\tilde{V}(q)]_{\text{Coulomb}} \\ \equiv m_Q - \mu_f \sum_{n=0} l_n(\mu_f/\mu) \alpha_s(\mu)^{n+1}, \quad (2.3)$$

where

$$[\tilde{V}(q)]_{\text{Coulomb}} = -\frac{4\pi\alpha_s}{q^2} \tilde{v}_c(\alpha_s, q/\mu) \quad (2.4)$$

is the Coulomb potential in momentum space defined as a PNRQCD coefficient function as discussed above. The coefficients $l_{0,1,2}$ are given in [29]. The large- β_0 estimate is easily derived from [36] and I will use the result for l_3 below. Because the Coulomb potential is scale-dependent at order α_s^4 and beyond, it depends on the PNRQCD matching scale. The coefficients l_n , $n > 2$, inherit this scale, which has to be specified in addition to μ_f . We can choose this scale equal to μ_f , so that the logarithm in the Coulomb potential [20] does not contribute to the PS mass.

In asymptotic counting $l_n \sim n! \mu/\mu_f$, so that the combination $m_Q k_n - \mu_f l_{n-1}$, which appears in the relation of $m_{Q,\text{PS}}$ to \bar{m}_Q , is convergent as desired. This is true for any $\mu_f > \text{few} \times \Lambda_{\text{QCD}}$. To satisfy $\delta m_Q \sim m_Q v^2$ or smaller, μ_f must not be parametrically larger than $m_Q v$. It is useful to choose μ_f of order $m_Q v \sim m_Q \alpha_s$. Note that this implies that $m_Q k_n$ and $\mu_f l_{n-1}$ are of different order in α_s , but cancel asymptotically.

2.3 1S mass

The 1S scheme was proposed in [37] and uses one half of the perturbative $\Upsilon(1S)$ mass as quark mass parameter. The perturbative $\Upsilon(1S)$ mass is related to the physical $\Upsilon(1S)$ mass $M_{\Upsilon(1S)}$ by

$$M_{\Upsilon(1S)} = 2m_{Q,1S} + \bar{\Lambda}_\Upsilon, \quad (2.5)$$

where $\bar{\Lambda}_\Upsilon$ is a poorly known non-perturbative contribution, which is most likely less (if not considerably less) than 100–150 MeV. (Some versions of the 1S scheme eliminate the bottom quark mass in favour of the physical $\Upsilon(1S)$ mass, the advantage being that the input parameter is a physical quantity which is very accurately measured. I prefer the version stated above, because

it does not obscure the presence of an unknown non-perturbative contribution. The 1S scheme can also be defined for top quarks [38]. It uses the perturbative toponium 1S mass under the assumption of a stable top.) Parametrically $\bar{\Lambda}_\Upsilon$ is of order $(\Lambda_{\text{QCD}}/(m_Q v))^4$ and not of order Λ_{QCD} . This guarantees that $m_{Q,1S}$ is less long-distance sensitive than the pole mass for perturbative $Q\bar{Q}$ systems.

The 1S scheme does not have an explicit subtraction scale μ_f , but it is similar (up to “finite” renormalizations) to the PS scheme with μ_f of order $m_Q\alpha_s$. The series expansion is

$$m_{Q,1S}/m_Q = 1 - \alpha_s \sum_{n=0} e_n(\mu) \alpha_s(\mu)^{n+1}. \quad (2.6)$$

The coefficients are known exactly up to e_2 [39] and will be given in Sect. 3.1 below. The asymptotic counting is $e_n \sim n! \mu/(m_Q\alpha_s)$, where the factor $\mu/(m_Q\alpha_s)$ follows from the fact that the physical scale is of order $m_Q\alpha_s$. Hence the combination $k_n - e_{n-1}\alpha_s$, which enters the relation of $m_{Q,1S}$ and \bar{m}_Q as coefficient at order α_s^n forms a convergent series with coefficients of order 1. As expected from the correspondence to $\mu_f \sim m_Q\alpha_s$, one has to combine coefficients of different order in α_s [37].

Strictly speaking the 1S scheme cannot be consistently used in NNLO (that is, keeping $e_2\alpha_s^4$ in (2.6)) and beyond for bottom quarks, since the $\Upsilon(1S)$ ultrasoft scale $m_Q\alpha_s^2$ is of order Λ_{QCD} . As discussed in Sect. 1.5, in this case the leading ultrasoft contribution (which would be order α_s^5 for a perturbative system) is non-perturbative and of the same parametric order as the term $e_2\alpha_s^4$. This should be kept in mind, but in the following I use (2.6) as a formal definition of the scheme, including the NNLO term e_2 .

2.4 Kinetic mass

The so-called kinetic mass has its roots in B physics [40]. The B meson mass has the heavy quark expansion

$$m_B = m_b + \bar{\Lambda} + \frac{\mu_\pi^2 - \mu_G^2}{2m_b} + \dots, \quad (2.7)$$

with μ_π^2 and μ_G^2 related to the matrix elements of the kinetic energy and chromo-magnetic operators, respectively. The kinetic mass can be un-

derstood as a perturbative evaluation of this formula, in which the matrix elements include loop momentum integration regions below the scale μ_f :

$$m_Q = m_{Q,\text{kin}}(\mu_f) + [\bar{\Lambda}(\mu_f)]_{\text{pert}} + \left[\frac{\mu_\pi^2(\mu_f)}{2m_Q} \right]_{\text{pert}} + \dots \quad (2.8)$$

The matrix elements on the right hand side subtract the long-distance sensitive contributions to the pole mass order by order in μ_f/m_Q and α_s . While easily stated, the definition of power divergent matrix elements in perturbation theory is largely arbitrary. The convention for the kinetic mass used in the literature uses an indirect definition through heavy flavour sum rules [40], which is rather complicated when compared with the other two mass definitions above. The relation between the kinetic and the pole mass is known exactly at order α_s^2 (including terms of order μ_f^2/m_Q) and in the large- β_0 limit at order α_s^3 [41].

2.5 Comparison

In table 1 I compare the various mass definitions for b quarks numerically using the $\overline{\text{MS}}$ mass as a reference parameter. Each entry gives the value of the mass using a 1-loop/2-loop/3-loop/4-loop relation. For reasons that will become clear later it is interesting to have four-loop accuracy. Where available I have used large- β_0 estimates to obtain the four-loop value. I used $\alpha_s(\bar{m}_b)$ as perturbative expansion parameter (with one exception, see below). In defining the kinetic mass, terms of order $(\mu_f/m_b)^3$ or less are dropped. At order α_s^3 the large- β_0 estimate is used, dropping all known terms that are subleading in this limit. (The relevant formula is given in the preprint version of [41].)

The 1S mass is computed in two different ways. First, I express it as a series in $\alpha_s(\bar{m}_b)$ with coefficients $k_n - e_{n-1}\alpha_s(\bar{m}_b)$ as explained above. A 4-loop relation then requires e_3 , which is not yet known, or at least its large- β_0 value. This result is shown in brackets in table 1. The second way first computes the PS mass at the scale $\mu_f = 2 \text{ GeV}$ as series in $\alpha_s(\bar{m}_b)$ and then relates the 1S mass to the PS mass as an expansion in $\alpha_s(2 \text{ GeV})$. In this case e_3 is not needed.

\overline{m}_b	$m_{b,\text{PS}}(2 \text{ GeV})$	$m_{b,\text{kin}}(1 \text{ GeV})$	$m_{b,1S}$	$m_{b,\text{pole}}$
$\alpha_s(m_Z) = 0.118$ [$\alpha_s(4.25 \text{ GeV}) = 0.2240$]				
4.15	4.36/4.44/4.47/4.48	4.41/4.49/4.50/-	4.36(50)/4.60(62)/4.67(66)/4.66(-)	4.55/4.75/4.89/5.04
4.20	4.41/4.49/4.52/4.54	4.46/4.54/4.56/-	4.41(55)/4.66(68)/4.72(72)/4.71(-)	4.60/4.80/4.95/5.09
4.25	4.46/4.55/4.58/4.59	4.52/4.60/4.61/-	4.46(61)/4.71(73)/4.78(77)/4.76(-)	4.65/4.85/5.00/5.15
4.30	4.52/4.60/4.64/4.65	4.57/4.65/4.67/-	4.52(66)/4.76(78)/4.83(82)/4.82(-)	4.71/4.91/5.06/5.20
4.35	4.57/4.66/4.69/4.70	4.62/4.71/4.72/-	4.57(71)/4.82(84)/4.88(88)/4.87(-)	4.76/4.96/5.11/5.25
$\alpha_s(m_Z) = 0.121$ [$\alpha_s(4.25 \text{ GeV}) = 0.2355$]				
4.15	4.37/4.45/4.49/4.51	4.42/4.51/4.52/-	4.37(52)/4.63(65)/4.70(69)/4.68(-)	4.57/4.79/4.96/5.14
4.20	4.42/4.51/4.55/4.56	4.48/4.56/4.58/-	4.42(57)/4.68(70)/4.75(75)/4.73(-)	4.62/4.84/5.01/5.19
4.25	4.47/4.56/4.61/4.62	4.53/4.62/4.64/-	4.47(62)/4.73(76)/4.81(80)/4.79(-)	4.67/4.90/5.07/5.25
4.30	4.53/4.62/4.66/4.67	4.58/4.67/4.69/-	4.53(68)/4.79(81)/4.86(85)/4.84(-)	4.73/4.95/5.12/5.30
4.35	4.58/4.68/4.72/4.73	4.64/4.73/4.75/-	4.58(73)/4.84(86)/4.92(91)/4.89(-)	4.78/5.00/5.18/5.35

Table 1: Comparison of b quark masses for given $\overline{\text{MS}}$ mass \overline{m}_b at the scale \overline{m}_b for two values of $\alpha_s(m_Z)$. We used $n_f = 4$ and put $m_c = 0$. Slanted numbers make use of large- β_0 estimates. All numbers in GeV.

The result is shown without brackets in table 1. The two ways of computing $m_{b,1S}$ correspond to the mass analyses performed in [42] and [43], respectively.

Except for the b quark pole mass all other masses given in the table are related to the $\overline{\text{MS}}$ mass by “convergent” series. The difference is clearly visible in the magnitude of successive perturbative terms. For the pole mass the minimal term is reached around 3-4 loops suggesting that its best accuracy cannot be smaller than about 150 MeV. On the contrary, the perturbative expansions of the other masses behave extremely well. At fourth order the error in relating them to \overline{m}_b is of order 10 MeV!

At this level, a comment on the effect of keeping the mass of internal charm quarks is necessary. Charm quark mass effects at order α_s^2 are known for the pole quark mass [32]. For given $\overline{m}_b = 4.25 \text{ GeV}$ and $\overline{m}_c = (1.1 - 1.4) \text{ GeV}$ the pole mass increases by about 8-10 MeV. The charm mass effect on the PS and 1S mass is easily computed in terms of the charm quark contribution to the photon vacuum polarization. I find, again for given \overline{m}_b , that $m_{b,\text{PS}}(2 \text{ GeV})$ and $m_{b,1S}$ are reduced by 11-12 MeV and 4-5 MeV respectively. These corrections could be applied to table 1, which is generated for $m_c = 0$. Charm effects at order α_s^3 and beyond are not known and introduce an error of perhaps 10 MeV. If the average internal loop momentum becomes small,

the charm quark decouples and one can switch to an effective description with only three light flavours [34].

2.6 Application: inclusive heavy quark decay

Before returning to $Q\bar{Q}$ systems it is interesting to see how these mass definitions fare in decays of B mesons. As an example consider the inclusive semi-leptonic B decay $B \rightarrow X_u l \nu$. Many more examples can be found in [37], though restricted to the 1S scheme. (An earlier 1-loop analysis with the kinetic mass was done in [44].)

It is known that inclusive B decays are less long-distance sensitive than the pole mass [28, 45] and so another mass parameter is warranted. But the situation is different from onium systems, because there is no scale other than m_b . Hence $\overline{m}_b(\overline{m}_b)$ is a legitimate choice. However, this works well only asymptotically but fails in low orders in α_s [46]. The decay rate, neglecting power corrections, is

$$\Gamma = \frac{G_F^2 |V_{ub}|^2 M^5}{192\pi^3} \left[1 - \delta_1 - \delta_2 + O(\alpha_s^3) \right]. \quad (2.9)$$

With the second order correction in the pole mass scheme from [47], the 1-loop and 2-loop correction in various other mass renormalization conventions is computed and shown in table 2. All “alternative” mass definitions introduced above do very well.

M	δ_1	δ_2
$m_{b,\text{pole}}$	+0.17	+0.10
\overline{m}_b	-0.30	-0.13
$m_{b,\text{PS}}(2\text{ GeV})$	-0.03	-0.01
$m_{b,1S}$	+0.11	+0.03
$m_{b,\text{kin}}(1\text{ GeV})$	+0.03	-0.005

Table 2: First and second order perturbative terms in inclusive $b \rightarrow u$ decay with various mass parameters.

It is perhaps not evident why this is the case given that there is no a priori reason not to use the $\overline{\text{MS}}$ mass. A plausible argument is that while the characteristic scale in inclusive $b \rightarrow u$ decay is parametrically of order m_b , it is numerically smaller [48]. This forces the b quark closer to its mass shell although not close enough to justify the use of the pole mass. Similar improvements by using “alternative” mass renormalization schemes occur for other heavy quark decays [37].

3. Quarkonium

In this section I review results on quarkonium bound states. Unfortunately, none of the observed charmonium and bottomonium states is truly perturbative, i.e. satisfies $m_Q v^2 \gg \Lambda_{\text{QCD}}$. The best candidate to try our theory are the $\Upsilon(1S)$ and η_b states. Higher excitations are almost certainly non-perturbative, although more non-relativistic.

3.1 Masses

The quarkonium binding energy is of order $m_Q \alpha_s^2$ in leading order. For an arbitrary $Q\bar{Q}[nl]$ state the energy is known to order α_s^4 [39]. For nS states the result of [39] has been confirmed by [49, 50, 16]. The $\Upsilon(1S)$ mass, expressed in terms of the b quark pole mass, is given by

$$M_{\Upsilon(1S)} = 2m_b - \frac{4}{9} m_b^2 \alpha_s^2 \left[1 + \frac{\alpha_s}{\pi} \left(-\frac{25}{6} l + \frac{203}{18} \right) + \frac{\alpha_s^2}{\pi^2} \left(\frac{625}{48} l^2 - \frac{1429}{24} l - \frac{9\pi^4}{32} + \frac{2453\pi^2}{216} + \frac{1235\zeta(3)}{36} + \frac{7211}{108} \right) \right]$$

$$= 2m_b - \frac{4}{9} m_b^2 \alpha_s^2 \left[1 + 1.08 + 1.76 \right], \quad (3.1)$$

where $l = \ln(16m_b^2 \alpha_s^2 / (9\mu^2))$ and $\alpha_s = \alpha_s(\mu)$ and the second line is given for μ such that $l = 0$ (for $m_b = 5\text{ GeV}$), in which case $\alpha_s(\mu) = 0.30$. Corrections to this result are order α_s^5 and order

$$\alpha_s^2 \left(\frac{\Lambda_{\text{QCD}}}{m_b \alpha_s} \right)^2 \left(\frac{\Lambda_{\text{QCD}}}{m_b \alpha_s^2} \right)^{2+2n} \quad (3.2)$$

from the operator product expansion [24].

An interesting application of (3.1) is to use it to determine the b quark mass. The non-convergence of the series (3.1) seems to make this impossible. However, if the series is expressed in terms of the PS mass or the $\overline{\text{MS}}$ mass, the convergence is dramatically improved as seen from the column referring to $m_{b,1S}$ in table 1. In [43] this has been used to obtain

$$\overline{m}_b(\overline{m}_b) = (4.24 \pm 0.09)\text{ GeV}. \quad (3.3)$$

The central value is obtained by varying μ from 1.25 GeV to 4 GeV and by symmetrizing the error. The total error is dominated by the unknown non-perturbative contribution from ultrasoft gluons and the fact that the OPE series in n of (3.2) may not converge. Note that (3.3) uses the 4-loop relation in table 1 because the series (3.1) in terms of the PS or $\overline{\text{MS}}$ mass is convergent in asymptotic counting and hence determines the quark mass to order α_s^4 . This is the main reason why (3.3) differs substantially from the value obtained in [39], where \overline{m}_b is determined via the b pole mass and by a 2-loop relation.

There exist partial results at order α_s^5 which may be used to estimate the perturbative error on $M_{\Upsilon(1S)}$. The mass correction from ultrasoft gluon exchange has been obtained in [51]:

$$\delta M_{\Upsilon(1S)}^{us} = 6.31 m_b \alpha_s^5 \left[\ln \left(\frac{9\mu_{us}}{8m_b \alpha_s^2} \right) - 2.06 \right] \approx -(35 - 250)\text{ MeV}. \quad (3.4)$$

To obtain the estimate for the ultrasoft constant terms, I interpreted α_s^5 as $\alpha_s(\mu_1)^4 \alpha_s(\mu_{us})$, with $\mu_1 \approx 2\text{ GeV}$ the scale that makes the logarithm l in (3.1) vanish, and varied μ_{us} from 0.7 GeV to 2 GeV. The numerical estimate is highly sensitive to the PNRQCD cut-off scale μ_{us} which must cancel in a complete order α_s^5 calculation.

The second estimate is based on the logarithmically enhanced terms of order $\alpha_s^5 \ln \alpha_s$ [21, 52]:

$$\begin{aligned} \delta M_{\Upsilon(1S)}^{ln} &= \frac{1730}{81\pi} m_b \alpha_s^5 \ln(1/\alpha_s) \\ &\approx (75 - 100) \text{ MeV}. \end{aligned} \quad (3.5)$$

Here I varied the scale in $\alpha_s \ln(1/\alpha_s)$ from 0.7 to 2 GeV as above. This set of terms does not depend on arbitrary cut-offs, but the logarithm is not large. Note that the coefficient of the logarithm is not identical to the one in (3.4), because there are logarithms unrelated to ultrasoft effects in the potentials of PNRQCD.

Both corrections may not be small compared to the error estimate in (3.3), but since they come with opposite sign and constitute only part of the α_s^5 correction it is too early to revise (3.3). However, they illustrate that next-to-next-to-next-to-leading order effects may be large.

3.2 Decay into a lepton pair

The decay of a nS state into l^+l^- measures the quarkonium wave function $\Psi(0)$ at the origin. In turn, this parameter enters all those quarkonium decays which proceed through $Q\bar{Q}$ annihilation. In terms of the quark electric charge e_Q , the fine structure constant α and the mass M_{nS} of the quarkonium, the decay rate reads, for massless leptons:

$$\Gamma = \frac{16\pi e_Q^2 \alpha^2}{M_{nS}^2} C(\alpha_s; \mu)^2 |\Psi(0)|^2(\mu). \quad (3.6)$$

Here $C(\alpha_s; \mu)$ is the short-distance coefficient of the non-relativistic vector current $\psi^\dagger \sigma^i \chi$, which is known to NNLO [22, 23], and $\Psi(0)$ is related to the NRQCD matrix element of the current. Note that the wave function at the origin is factorization scale dependent at NNLO. Eq. (3.6) neglects corrections from higher dimension operators. They are incorporated in the numerical result below.

The short-distance coefficient is poorly convergent in the $\overline{\text{MS}}$ factorization scheme implied by the threshold expansion. Numerically, at the NRQCD matching scale $\mu_h = m_Q$,

$$\begin{aligned} C(\alpha_s; m_Q) &= 1 - 0.849 \alpha_s(m_Q) \\ &- (4.51 - 0.042n_f) \alpha_s(m_Q)^2 + \dots, \end{aligned} \quad (3.7)$$

where n_f refers to all lighter flavours, approximating them as massless. This provided the first hint that NNLO corrections to $Q\bar{Q}$ systems are very large [22].

The coefficient function is scheme-dependent and the large NNLO correction may be a scheme artefact. For perturbative $Q\bar{Q}$ systems one can also compute $|\Psi(0)|^2(\mu)$ in PNRQCD perturbation theory (which implies treating the Coulomb interaction non-perturbatively). The NNLO α_s^5 correction to $|\Psi(0)|^2(\mu)$ has been obtained analytically in [50] and has been confirmed by [16]. (Note, however, that the result is not presented explicitly in [16]. In [49] a more complicated representation is given. According to [49] the two representations agree numerically.) The decay width for $\Upsilon(1S) \rightarrow l^+l^-$ to NNLO in PNRQCD perturbation theory, including the higher dimension operators mentioned above, reads

$$\begin{aligned} \Gamma(\Upsilon(1S) \rightarrow l^+l^-) &= \frac{32}{27} e_b^2 \alpha^2 m_b \alpha_s(\mu)^3 \left[1 + \right. \\ &(-1.99l - 2.00) \alpha_s(\mu) + (2.64l^2 + 3.26l \\ &\left. + 11.19 + 7.43 \ln(m_b/\mu)) \alpha_s(\mu)^2 \dots \right], \end{aligned} \quad (3.8)$$

where l is defined as in (3.1). The logarithm of m_b/μ is partly related to the fact that the natural scale in the short-distance coefficient is m_b and not μ_1 . However, a consistent treatment of all such logarithms requires renormalization group methods and has not yet been given. For μ_1 such that $l = 0$ (with $m_b = 5$ GeV), the factor in brackets is

$$F(\mu_1) = 1 - 0.60 + 1.63. \quad (3.9)$$

As in (3.1) the series is not convergent at all. We have been able to eliminate such behaviour as unphysical for the quarkonium mass, but we cannot apply the same reasoning here. It therefore seems that the leptonic decay width cannot be predicted reliably in perturbation theory.

Despite (3.7) bottomonium and charmonium decays may well be reliably predicted in NRQCD with the NRQCD matrix elements treated as non-perturbative parameters. To obtain a definite conclusion one would have to compute another quarkonium decay, such as $\eta_b \rightarrow \gamma\gamma$ or $\Upsilon(1S) \rightarrow$ light hadrons, to NNLO. The ratio of decay rates

is given by a factorization scheme independent ratio of short-distance coefficients. It may be that such ratios are more convergent than (3.7).

A subset of next-to-next-to-next-to-leading order contributions to the $\Upsilon(1S)$ leptonic decay width is known. The ultrasoft correction at order α_s^6 contributes

$$\begin{aligned} \delta F^{us} &= -6.81\alpha_s^3 \left[\ln \left(\frac{9\mu_{us}}{8m_b\alpha_s^2} \right) - 0.777 \right] \\ &\approx (-0.15) - (+0.09). \end{aligned} \quad (3.10)$$

to F in (3.9) [51]. The numerical range is computed with the same prescription used for (3.4). The leading logarithmic contribution at order α_s^6 is a double logarithm. It arises as a product of an ultrasoft or potential logarithm and a logarithm related to the anomalous dimension of the current $\psi^\dagger\sigma^i\chi$. The correction is [52]:

$$\begin{aligned} \delta F^{ln} &= -\frac{212}{9\pi}\alpha_s^3 \ln(1/\alpha_s)^2 \\ &\approx -(0.08 - 0.30). \end{aligned} \quad (3.11)$$

The numerical range is computed with the same prescription used for (3.5). Again these corrections are not small, but their impact is less severe given the already large uncertainty of $F(\mu_1)$ in (3.9).

In conclusion, higher order corrections almost always turn out to be large. The $\Upsilon(1S)$ mass may be useful to determine the b quark mass. A reliable prediction of absolute decay widths appears improbable, but it remains to be checked whether ratios behave better. This conclusion may be frustrating. However, the numerical analysis of the quarkonium mass and wave function at the origin provides important insight into the structure of corrections to inclusive top and bottom quark pair production near threshold.

4. Top quark pair production near threshold

Top quark pair production is one of the major physics cases for a first linear e^+e^- collider and has been studied extensively in this context [53]. The threshold behaviour of the cross section can be used to determine the top quark mass with

great precision – provided the theoretical prediction is accordingly accurate.

Toponium would be the perfect candidate for perturbative applications of non-relativistic QCD, but nature has provided another complication. The electroweak decay width $\Gamma_t \approx \Gamma(t \rightarrow bW)$ increases as m_t^3 . In the standard model $\Gamma_t \approx 1.4$ GeV, of the same order of magnitude as the ultrasoft scale of toponium [54].

Suppose (for a moment) that the top quark is stable and neglect the axial-vector coupling to the Z boson, which is suppressed near threshold. Then the $t\bar{t}$ production cross section is obtained from the correlation function

$$\begin{aligned} \Pi_{\mu\nu}(q^2) &= (q_\mu q_\nu - q^2 g_{\mu\nu}) \Pi(q^2) \\ &= i \int d^4x e^{iq \cdot x} \langle 0 | T(j_\mu(x) j_\nu(0)) | 0 \rangle, \end{aligned} \quad (4.1)$$

where $j^\mu(x) = [\bar{t}\gamma^\mu t](x)$ is the top quark vector current and $s = q^2$ the centre-of-mass energy squared. Defining the usual R -ratio $R = \sigma_{t\bar{t}}/\sigma_0$ ($\sigma_0 = 4\pi\alpha_{em}^2/(3s)$, where α_{em} is the electromagnetic coupling at the scale $2m_t$), the relation is

$$R = \frac{4\pi e_t^2}{s} (1 + a_Z) \text{Im} \Pi^{ii}(s + i\epsilon), \quad (4.2)$$

where $e_t = 2/3$ is the top quark electric charge in units of the positron charge and a_Z accounts for the vector coupling to the Z boson. (For the remainder of this section, I set $a_Z = 0$ for simplicity.) Only the spatial components of the currents contribute up to NNLO. In the following m_t refers to the top quark pole mass.

At leading order in PNRQCD perturbation theory the heavy quark current two-point function is given by the first diagram in figure 4. The $t\bar{t}$ pair is created by the current, interacts instantaneously through the (leading order) Coulomb potential, and is annihilated by the current. Figure 4 is actually misleading. Because $t\bar{t}$ production is short-distance compared to the toponium scale $m_t\alpha_s$, the pair is created and destroyed at the same space-time point! The leading order result is

$$\Pi(s) = \frac{3}{2m_t^2} G_c(0, 0; E), \quad (4.3)$$

where $E = \sqrt{s} - 2m_t$. The Green function at the origin is ultraviolet divergent. In dimensional

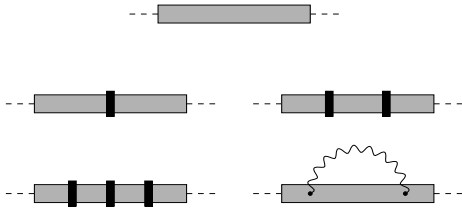


Figure 4: PNRQCD perturbative diagrams for the heavy quark current correlation function. At leading order the current generates a $Q\bar{Q}$ pair which propagates with the Coulomb Green function (first line). Black bars denote insertions of potentials. The last diagram contains an ultrasoft gluon exchange. Both diagrams in the last line are beyond NNLO.

regularization, with $\overline{\text{MS}}$ subtractions, one finds

$$G_c(0,0;E) = -\frac{m_t^2 \alpha_s}{3\pi} \left[\frac{1}{2\lambda} + \frac{1}{2} \ln \frac{-4m_t E}{\mu^2} - \frac{1}{2} + \gamma_E + \psi(1-\lambda) \right], \quad (4.4)$$

where $\lambda = 2\alpha_s/(3\sqrt{-E/m_t})$ and γ_E is Euler's constant. The cross section requires only the discontinuity of Π , which is scheme-independent. The Green function contains a continuum at $E > 0$ and poles at $E < 0$, from which the energy and wave function at the origin of toponium resonances can be extracted.

How does the top decay width affect this result? For top quarks with energy $E \sim m_t v^2 \sim \Gamma_t$ and momentum $\vec{p} \sim m_t v$, we can approximate the quark propagator (in the potential region)

$$\frac{1}{\not{P}_t - m_t - \Sigma(P_t)} \approx \frac{1}{E + i\Gamma_t - \vec{p}^2/(2m_t)} [1 + \mathcal{O}(v)]. \quad (4.5)$$

As expected, the width is a leading order effect, but can be taken into account at this order by substituting $E \rightarrow \bar{E} \equiv E + i\Gamma_t$, where Γ_t is the gauge-independent on-shell decay width. This gives the classic leading order result of [55]. Because the Green function is evaluated off the real axis, the toponium poles are smeared out. For $\Gamma_t \approx 1.4 \text{ GeV}$, we expect to see a broad remnant of the $1S$ pole, but all higher resonances overlap and form a continuum.

Next-to-leading order corrections to this result have been known for some time [56]. Other

properties of the production process, such as top quark momentum distributions and asymmetries generated by interference of vector and axial-vector contributions, have been studied in some detail [57], sometimes with non-perturbative modifications of the heavy quark potential that have little justification in the theoretical framework described in earlier sections. The recent development concerns the calculation of NNLO corrections in a systematic non-relativistic approach [58, 16, 59, 38, 60]. In PNRQCD Feynman diagrams these corrections are given by the two diagrams in the second line of figure 4 with potentials up to NNLO. These diagrams correspond to integrals of the form

$$\int \frac{d^3 \vec{p}}{(2\pi)^3} \frac{d^3 \vec{p}'}{(2\pi)^3} \frac{d^3 \vec{q}_1}{(2\pi)^3} \frac{d^3 \vec{q}_2}{(2\pi)^3} \tilde{G}_c(\vec{p}, \vec{q}_1; \bar{E}) \cdot \delta V(\vec{q}_1 - \vec{q}_2) \cdot \tilde{G}_c(\vec{q}_2, \vec{p}'; \bar{E}) \quad (4.6)$$

and generalizations with more than one insertion of an interaction potential δV . Triple insertions of potentials and ultrasoft gluon exchange are higher order and neglected. The new calculations either employ a combination of numerical and analytical methods [58, 59, 38] or are fully analytical [16, 60]. The numerical solution of the Schrödinger equation contains higher order corrections, because an infinite number of insertions of the potentials that are kept in the equation is included. This could be an advantage if it could be argued that these higher order corrections are the dominant ones.

The first NNLO calculations [58] reported large corrections to the peak position and normalization of the remnant of the $1S$ toponium resonance. The correction to the peak position could be explained as an artefact of on-shell renormalization of the top quark mass [29]. Subsequent calculations incorporated this observation [16, 59, 38] and used one or the other of the ‘‘alternative’’ mass definitions discussed in Sect. 2. The NNLO pair production cross section near threshold in the PS scheme is shown in the upper panel of figure 5. For comparison the result in the pole mass scheme is shown in the lower panel – for the very last time!

The generic features of figure 5 are easily understood in terms of the results of Sect. 3, since

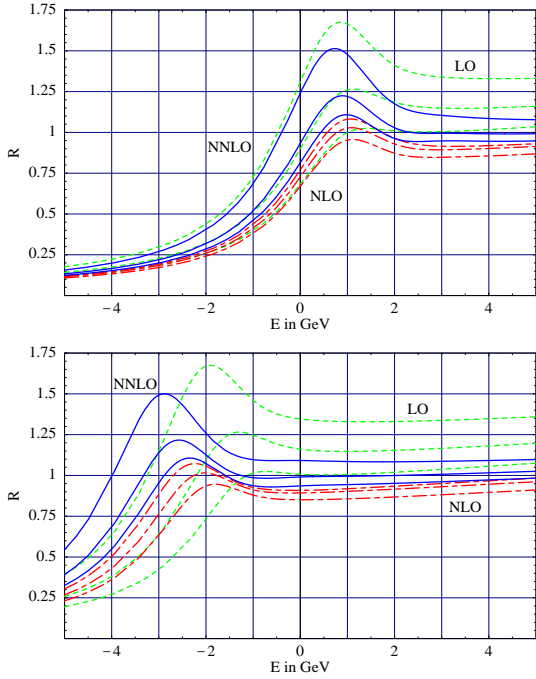


Figure 5: (a) [upper panel]: The normalized $t\bar{t}$ cross section (virtual photon contribution only) in LO (short-dashed), NLO (short-long-dashed) and NNLO (solid) as function of $E = \sqrt{s} - 2m_{t,\text{PS}}(20 \text{ GeV})$ (PS scheme, $\mu_f = 20 \text{ GeV}$). Input parameters: $m_{t,\text{PS}}(20 \text{ GeV}) = \mu_h = 175 \text{ GeV}$, $\Gamma_t = 1.40 \text{ GeV}$, $\alpha_s(m_Z) = 0.118$. The three curves for each case refer to $\mu = \{15(\text{upper}); 30(\text{central}); 60(\text{lower})\} \text{ GeV}$. (b) [lower panel]: As in (a), but in the pole mass scheme. Hence $E = \sqrt{s} - 2m_t$. Other parameters as above with $m_{t,\text{PS}}(20 \text{ GeV}) \rightarrow m_t$. Plot from [16]

the behaviour of successive perturbative approximations in the vicinity of the peak reflects essentially the perturbative expansion of the toponium $1S$ mass and wave function at the origin. The difference in the shift of the peak position in the pole and PS scheme is a direct consequence of the improved convergence of the perturbative expansion of M_{1S} . The stability of the peak position in the PS scheme implies that the PS mass (but not the pole mass) can be determined accurately from the measurement of the cross section. The PS mass determined in this way can also be related more reliably to the top quark \overline{MS} mass, which is probably the most useful reference parameter. The numerics of table 1 adapted to the top quark gives, for given $\overline{m}_t = 165 \text{ GeV}$ (and

$\alpha_s(\overline{m}_t) = 0.1083$):

$$m_t = [165.0 + 7.58 + 1.62 + 0.51 + 0.24 (\text{est.})] \text{ GeV} \quad (4.7)$$

$$m_{t,\text{PS}}(20 \text{ GeV}) = [165.0 + 6.66 + 1.20 + 0.28 + 0.08 (\text{est.})] \text{ GeV}, \quad (4.8)$$

where the numbers refer to successive terms in the perturbative expansion. The difference in convergence is significant on the scale of 0.1 GeV set by the projected statistical uncertainty on the mass measurement.

However, the perturbative expansion (3.8) for the wave function at the origin squared remains poorly convergent even for quarks as heavy as top. This leads to a large modification of the normalization of the cross section near the resonance peak at NNLO and also to a large renormalization scale dependence since the NNLO correction is proportional to α_s^5 . The recent calculations [16, 59, 38] agree qualitatively on the behaviour of the peak position and normalization. When the Schrödinger equation is solved numerically, the scale dependence of the peak normalization appears to be smaller than in figure 5 [38]. It is an open question which of the two scale dependences provides a realistic estimate of the present theoretical uncertainty.

A word of reservation applies to the term “NNLO”. All current NNLO calculations account for the width of the top quark by the replacement $E \rightarrow E + i\Gamma_t$ or a prescription of similar parametric accuracy. Beyond a leading order treatment of (4.5), counting $\Gamma_t \sim m_t v^2$, the self-energy has to be matched to better accuracy. The correction terms relate to the off-shell self-energy and carry electroweak gauge-dependence. A complete NNLO result in the presence of a width that scales as above therefore includes electroweak vertex corrections as well as single resonant backgrounds and non-factorizable corrections to the physical $WWb\bar{b}$ final state. Although some non-factorizable corrections are known near threshold [61] and away from threshold [62], a systematic treatment of these complications has not been attempted yet. Strictly speaking, the concept of the $t\bar{t}$ cross section is not defined at NNLO and the problem has to be formulated in terms of a particular final state such as $WWb\bar{b}$.

One may expect that single-resonant and non-factorizable corrections are ‘structureless’, that is, do not exhibit a pronounced resonance peak. In this case, they would add to the already existing normalization uncertainty, but would affect little the top quark mass measurement.

Besides the total cross section, top quark momentum distributions [59, 38] and vector-axial-vector interference [60] have been investigated. These quantities are even more delicate in the presence of a finite top quark width, which deserves further investigation. Top quark production near threshold in $\gamma\gamma$ collisions was considered in [63]. The theoretical accuracy is less in this case, because the two-loop short-distance coefficient has not yet been calculated.

How large could the corrections to figure 5 be? A particularly interesting set of corrections is again related to the ultrasoft scale. If we define the ultrasoft scale as the scale where the logarithm in (3.4) vanishes, we obtain $\mu_{us} \approx 3$ GeV for top quarks. The scale μ_1 at which l in (3.1) vanishes is 32.6 GeV. I then repeat the estimates (3.4), (3.5), (3.10) and (3.11) for top quarks, using again the results of [21, 51, 52], and varying μ_{us} between 2 GeV and 5 GeV. I obtain

$$\delta M_{1s}^{us} \approx -(140 - 300) \text{ MeV} \quad (4.9)$$

$$\delta F^{us} \approx 0.01 - 0.05 \quad (4.10)$$

for the ultrasoft correction and

$$\delta M_{1s}^{ln} \approx (150 - 160) \text{ MeV} \quad (4.11)$$

$$\delta F^{ln} \approx -0.07 \quad (4.12)$$

for the leading logarithmic NNNLO correction. These numbers are relevant to $t\bar{t}$ production in the vicinity of the resonance peak. The corrections to the peak position are again not small compared to the residual uncertainty of about 200 MeV in figure 5, but the two corrections are of opposite sign and a conclusive estimate requires further NNNLO terms. In addition, one may worry about finite width effects in ultrasoft contributions.

To conclude this section, let me make the following remark. It is often said that the width of the top quark screens non-perturbative QCD effects and makes the threshold cross section calculable in perturbative QCD. It is true that the

width smears the toponium resonances and converts the observed cross section into a smooth excitation curve. However, it is not true that the top quark width screens non-perturbative effects any more than the existence of a perturbative ultrasoft scale $m_t \alpha_s^2 \sim \Gamma_t$ already does. Even for stable top quarks the production cross section near threshold (averaged over an interval several times Λ_{QCD}) is perturbatively calculable, as would be the toponium resonances and their decays. Interestingly, perturbative resummation with power counting $v \sim \alpha_s$ seems to make sense even as $v \rightarrow 0$ at fixed α_s . In particular, the cross section directly at threshold seems to be infrared safe in perturbation theory. As $v \rightarrow 0$ the arguments of the coupling constants $\alpha_s(m_Q v)$ and $\alpha_s(m_Q v^2)$ freeze at values of order $m_Q \alpha_s$ and $m_Q \alpha_s^2$, respectively, and do not tend to zero. This has been checked explicitly by investigating the logarithms up to order α_s^3 (NNLO).

5. Sum rules, the b quark mass

As a final application we return to the b quark mass. There are legitimate doubts concerning the reliability of (3.3) given that $\Upsilon(1S)$ is hardly a truly perturbative onium. One can by-pass this problem by considering averages over the bottom pair production cross section rather than exclusive resonances. This leads us to consider sum rules [64]

$$\begin{aligned} M_n / (10 \text{ GeV})^{2n} &\equiv \frac{12\pi^2}{n!} \frac{d^n}{d(q^2)^n} \Pi(q^2) \Big|_{q^2=0} \\ &= \int_0^\infty \frac{ds}{s^{n+1}} R_{b\bar{b}}(s) \end{aligned} \quad (5.1)$$

which equate an experimental average of the cross section to the perturbatively computable derivatives (“moments”) of the bottom vector current correlation function.

The parameters of the lowest $\Upsilon(nS)$ resonances are well measured and one chooses n large enough that the experimental uncertainty on the continuum cross section is small compared to the theoretical uncertainty. This occurs for $n \geq 6$. For such moments the ordinary perturbative expansion of the moments breaks down and has

to be replaced by non-relativistic resummation and PNRQCD perturbation theory. Leading order and next-to-leading order analyses of the sum rule with non-relativistic resummation have been performed in [65] and [66], respectively. After integration over s the expansion of $R_{b\bar{b}}(s)$ in α_s/v turns into an expansion in $\alpha_s\sqrt{n}$. Non-relativistic resummation sums these terms to all orders. For moments the scale $m_b v$ turns into $2m_b/\sqrt{n}$; the ultrasoft scale $m_b v^2$ is m_b/n . The requirement that the ultrasoft scale is perturbative translates into $n \leq 10$. Larger moments are often used in the literature. This introduces a systematic uncertainty which is difficult to quantify at NNLO, since at this order ultrasoft corrections are not included.

Several NNLO calculations have been completed recently [49, 67, 50, 42, 43], the calculation being almost identical to that of top pair production near threshold. The later publications [50, 42, 43] abandoned the idea of determining the pole mass and usually extract the bottom $\overline{\text{MS}}$ mass \overline{m}_b . This is done by extracting the PS or 1S or kinetic mass from the sum rule, which is then converted into \overline{m}_b . Although the different groups compute the same quantity, there are differences in the implementation of the resummation which are formally beyond NNLO. These concern (a) whether the short-distance coefficient (3.7) is kept as an overall factor or multiplied out to NNLO; (b) whether the integral over s in (5.1) is done exactly or in a non-relativistic approximation; (c) whether the energy denominator of the full Green function is expanded up to NNLO or whether the exact NNLO energy levels are kept. These differences in implementation can shift the value of m_b extracted from the sum rule by up to 100 MeV.

Further differences arise in the choice of moments, renormalization scale, at which the sum rule is evaluated, and the analysis strategy.

Refs. [50, 43] perform essentially a single-moment analysis, based on the fact that the theoretical error is highly correlated between different moments. It is then checked that varying the moment gives a negligible difference. One then finds a significant renormalization scale uncertainty, which can be traced back to the badly behaved expansion (3.9). A typical result is shown

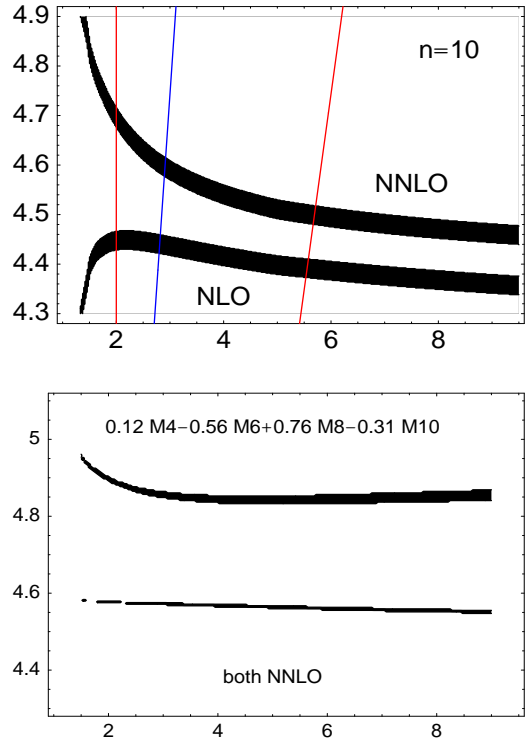


Figure 6: (a) [upper panel]: The value of $m_{b,\text{PS}}(2\text{ GeV})$ obtained from the 10th moment as a function of the renormalization scale in NLO and NNLO and for $\alpha_s(m_Z) = 0.118$. The dark region specifies the variation due to the experimental error on the moment. The middle line marks the scale $\mu_n = 2m_b/\sqrt{n}$, the two outer lines determine the scale variation from which the theoretical error is computed. Plot from [43]. (b) [lower panel]: The value of $m_{b,\text{PS}}(2\text{ GeV})$ obtained from a linear combination of moments as a function of the renormalization scale in NNLO. M_n is defined with the normalization of (5.1).

in the upper graph of figure 6. The results

$$m_{b,\text{PS}}(2\text{ GeV}) = (4.60 \pm 0.11)\text{ GeV} \quad [43] \quad (5.2)$$

$$m_{b,\text{kin}}(1\text{ GeV}) = (4.56 \pm 0.06)\text{ GeV} \quad [50] \quad (5.3)$$

differ by about 80 MeV, when related to each other according to table 1, but are consistent with each other within implementational differences. The larger error on the first result follows from a larger renormalization scale variation.

The analysis of [42] is different, because it uses linear combinations of moments. The linear combination chosen in [42] is less sensitive to a variation of the renormalization scale, while re-

Refs.	$\overline{m}_b(\overline{m}_b)$	m_b	Remarks
[50]	4.20 ± 0.10	--	Sum rules (via $m_{b,\text{kin}}(1 \text{ GeV})$)
[42, 68]	4.19 ± 0.06	--	Sum rules (via $m_{b,1S}$)
[43, 69]	4.26 ± 0.10	4.97 ± 0.17	Sum rules (via $m_{b,\text{PS}}(2 \text{ GeV})$)
[49]	4.21 ± 0.11	4.80 ± 0.06	Sum rules (via m_b , 2-loop)
[39]	4.44 ± 0.04	5.04 ± 0.09	$\Upsilon(1S)$ mass (via m_b , 2-loop)
[43]	4.24 ± 0.09	--	$\Upsilon(1S)$ mass (via $m_{b,\text{PS}}(2 \text{ GeV})$)
[68]	4.21 ± 0.07	--	$\Upsilon(1S)$ mass (direct)

Table 3: Bottom quark $\overline{\text{MS}}$ and pole mass values (in GeV) obtained from NNLO sum rule or $\Upsilon(1S)$ mass calculations.

taining sensitivity to m_b . This is illustrated in the lower panel of figure 6 in the PS scheme. In this way, [42] obtains

$$m_{b,1S} = (4.71 \pm 0.03) \text{ GeV}, \quad (5.4)$$

which is close to (5.3) after conversion. This result depends crucially on combining moments at identical renormalization scales rather than their “natural” scale $2m_b/\sqrt{n}$, and on discarding possible multiple solutions (as the upper one in figure 6b). In my opinion the error quoted in (5.4) should be understood as an error that follows under the specific assumptions of the analysis strategy. It can hardly be considered as a realistic estimate of the total theoretical error, given the differences that can arise in different implementations of the theoretical moments and given the size of ultrasoft effects discussed in Sect. 3.1.

The results quoted above can be converted into the bottom $\overline{\text{MS}}$ mass using table 1. A summary of NNLO results from sum rules and, for comparison, the $\Upsilon(1S)$ mass, is compiled in table 3, where I quote the number given by the authors. This number may differ from the one of table 1, because not always is a four-loop related to \overline{m}_b used as appropriate to a NNLO sum rule calculation (cf. the discussion after (3.3)). This difference is small when mass definitions with convergent relations to \overline{m}_b are used, see table 1, but affects \overline{m}_b when computed from the pole mass via a 2-loop relation. For this reason the results for \overline{m}_b from [39, 49] in table 3 should in fact be decreased by about 200 MeV. This makes [39] consistent with the other \overline{m}_b determinations, but puts the result of [49] off by

200 MeV. Comparison of pole mass results shows that this discrepancy is already present in the pole mass value before conversion to \overline{m}_b . The small pole mass value of [49] is a consequence of the fact that the sum rule is evaluated at high renormalization scales. Fig. 5a shows that this leads to reduction of m_b .

My “best” estimate for the b quark $\overline{\text{MS}}$ mass is a (potentially biased) combination of the results of [50, 42, 43]. It is remarkable that the sum rule result is consistent with the $\Upsilon(1S)$ results despite the fact that the systematics of non-perturbative effects and scale dependence is different. Nevertheless, the results of table 3 are not independent and may be affected by common, unidentified theoretical uncertainties. This being said, my preferred value is

$$\overline{m}_b(\overline{m}_b) = (4.23 \pm 0.08) \text{ GeV}. \quad (5.5)$$

This is in beautiful agreement with $\overline{m}_b(\overline{m}_b) = 4.26 \pm 0.07 \text{ GeV}$ [70] obtained from lattice HQET. This uses the B meson mass, a lattice calculation of the (properly defined) binding energy of the B meson in the unquenched, two-flavour approximation to heavy quark effective theory, and a two-loop perturbative matching to the $\overline{\text{MS}}$ scheme. To our knowledge, this is the only other NNLO determination of the $\overline{\text{MS}}$ mass besides the sum rule calculations mentioned above (which, in fact, are N^4LO as far as \overline{m}_b is concerned). In my opinion using an error smaller than 80 MeV on $\overline{m}_b(\overline{m}_b)$ or any of the “alternative” masses cannot be justified at present. Using smaller errors in B physics observables may have dangerous consequences for consistency checks of the

CKM model of CP violation.

6. Concluding remarks

The theory of perturbative onium systems has undergone an exciting transition from potential models with arbitrary cut-offs and poorly understood accuracy to a systematic effective theory description. This transition can be compared in significance with the development of heavy quark effective theory for B and D mesons. Unfortunately, nature has not been kind to us, leaving us with systems which are barely perturbative (bottomonium) or extremely short-lived (toponium).

Along with this development perturbative expansion tools have been invented and the most basic quantities are now computed to next-to-next-to-leading order. These calculations sharpened our understanding of heavy quark mass renormalization, but large corrections remain in most cases. They confront us with the challenge of a complete next-to-next-to-next-to-leading order calculation. With so many tools at hand, progress is surely expected.

Acknowledgments

I would like to thank the organizers of HF8 for making this a focused and enjoyable meeting. Thanks to A. Signer and V.A. Smirnov for collaboration on subjects related to this review and to A.H. Hoang and A. Pineda for discussions. This work was supported in part by the EU Fourth Framework Programme ‘Training and Mobility of Researchers’, Network ‘Quantum Chromodynamics and the Deep Structure of Elementary Particles’, contract FMRX-CT98-0194 (DG 12 - MIHT).

References

- [1] E. Eichten and B. Hill, *Phys. Lett.* **B234** (1990) 511; B. Grinstein, *Nucl. Phys.* **B339** (1990) 253; H. Georgi, *Phys. Lett.* **B240** (1990) 447.
- [2] N. Isgur and M.B. Wise, *Phys. Lett.* **B232** (1989) 113; **B237** (1990) 527.
- [3] W.E. Caswell and G.P. Lepage, *Phys. Lett.* **B167** (1986) 437.
- [4] B.A. Thacker and G.P. Lepage, *Phys. Rev.* **D43** (1991) 196; G.P. Lepage *et al.*, *Phys. Rev.* **D46** (1992) 4052
- [5] G.T. Bodwin, E. Braaten and G.P. Lepage, *Phys. Rev.* **D51** (1995) 1125; **D55** (1997) 5853 (E); I.Z. Rothstein, these proceedings [hep-ph/9911276].
- [6] A.V. Manohar, *Phys. Rev.* **D56** (1997) 230.
- [7] M. Beneke, *Non-relativistic effective theory for quarkonium production in hadron collisions in: The strong interaction, from hadrons to partons*, p. 549, Stanford 1996 [hep-ph/9703429].
- [8] P. Labelle, *Phys. Rev.* **D58** (1998) 093013 [hep-ph/9608491].
- [9] M. Luke and A.V. Manohar, *Phys. Rev.* **D55** (1997) 4129.
- [10] B. Grinstein and I.Z. Rothstein, *Phys. Rev.* **D57** (1998) 78.
- [11] M. Luke and M.J. Savage, *Phys. Rev.* **D57** (1998) 413.
- [12] M. Beneke and V.A. Smirnov, *Nucl. Phys.* **B522** (1998) 321.
- [13] H.W. Grieffhammer, *Phys. Rev.* **D58** (1998) 094027; *Power counting and beta function in NRQCD* [hep-ph/9810235].
- [14] A. Pineda and J. Soto, *Nucl. Phys. Proc. Suppl.* **64** (1998) 428 [hep-ph/9707481]; *Phys. Rev.* **D59** (1999) 016005.
- [15] M. Beneke, *New results on heavy quarks near threshold* [hep-ph/9806429].
- [16] M. Beneke, A. Signer and V.A. Smirnov, *Phys. Lett.* **B454** (1999) 137.
- [17] M.E. Luke, A.V. Manohar and I.Z. Rothstein, *Renormalization group scaling in non-relativistic QCD* [hep-ph/9910209].
- [18] Y. Schröder, *Phys. Lett.* **B447** (1999) 321.
- [19] T. Appelquist, M. Dine and I.J. Muzinich, *Phys. Lett.* **69B** (1977) 231; *Phys. Rev.* **D17** (1978) 2074.
- [20] N. Brambilla, A. Pineda, J. Soto and A. Vairo, *Phys. Rev.* **D60** (1999) 091502; *Potential NRQCD: An effective theory for heavy quarkonium* [hep-ph/9907240].
- [21] N. Brambilla, A. Pineda, J. Soto and A. Vairo, *The heavy quarkonium spectrum at order $m\alpha_s^5 \ln \alpha_s$* [hep-ph/9910238].
- [22] M. Beneke, A. Signer and V.A. Smirnov, *Phys. Rev. Lett.* **80** (1998) 2535.

- [23] A. Czarnecki and K. Melnikov, *Phys. Rev. Lett.* **80** (1998) 2531.
- [24] H. Leutwyler, *Phys. Lett.* **B98** (1981) 447; M.B. Voloshin, *Sov. J. Nucl. Phys.* **36**(1) (1982) 143; A. Pineda, *Nucl. Phys.* **B494** (1997) 213.
- [25] A.S. Kronfeld, *Phys. Rev.* **D58** (1998) 051501.
- [26] I.I. Bigi and N.G. Uraltsev, *Phys. Lett.* **B321** (1994) 412.
- [27] M. Beneke and V.M. Braun, *Nucl. Phys.* **B426** (1994) 301; M. Beneke, *Phys. Lett.* **B344** (1995) 341.
- [28] I.I. Bigi, M.A. Shifman, N.G. Uraltsev and A.I. Vainshtein, *Phys. Rev.* **D50** (1994) 2234.
- [29] M. Beneke, *Phys. Lett.* **B434** (1998) 115.
- [30] A.H. Hoang, M.C. Smith, T. Stelzer and S. Willenbrock, *Phys. Rev.* **D59** (1999) 114014; A. Pineda, *Heavy quarkonium and nonrelativistic effective theories*, PhD thesis, Barcelona (1998).
- [31] M.C. Smith and S.S. Willenbrock, *Phys. Rev. Lett.* **79** (1997) 3825.
- [32] N. Gray, D.J. Broadhurst, W. Grafe and K. Schilcher, *Z. Phys.* **C48** (1990) 673.
- [33] K.G. Chetyrkin and M. Steinhauser, *Short distance mass of a heavy quark at order α_s^3* [hep-ph/9907509].
- [34] M. Beneke and V.M. Braun, *Phys. Lett.* **B348** (1995) 513; P. Ball, M. Beneke and V.M. Braun, *Nucl. Phys.* **B452** (1995) 563.
- [35] See, for example, the review: M. Beneke, *Phys. Rep.* **317** (1999) 1.
- [36] U. Aglietti and Z. Ligeti, *Phys. Lett.* **B364** (1995) 75.
- [37] A.H. Hoang, Z. Ligeti and A.V. Manohar, *Phys. Rev. Lett.* **82** (1999) 277; *Phys. Rev.* **D59** (1999) 074017.
- [38] A.H. Hoang and T. Teubner, *Phys. Rev.* **D60** (1999) 114027.
- [39] A. Pineda and F.J. Yndurain, *Phys. Rev.* **D58** (1998) 094022.
- [40] I.I. Bigi, M.A. Shifman and N.G. Uraltsev, *Ann. Rev. Nucl. Part. Sci.* **47** (1997) 591.
- [41] A. Czarnecki, K. Melnikov and N. Uraltsev, *Phys. Rev. Lett.* **80** (1998) 3189.
- [42] A.H. Hoang, *1S and \overline{MS} bottom quark masses from Upsilon sum rules* [hep-ph/9905550].
- [43] M. Beneke and A. Signer, *The bottom \overline{MS} quark mass from sum rules at next-to-next-to-leading order* [hep-ph/9906476].
- [44] N.G. Uraltsev, *Int. J. Mod. Phys.* **A11** (1996) 515.
- [45] M. Beneke, V.M. Braun and V.I. Zakharov, *Phys. Rev. Lett.* **73** (1994) 3058; A. Sinkovics, R. Akhoury and V.I. Zakharov, *Phys. Rev.* **D58** (1998) 114025.
- [46] P. Ball, M. Beneke and V.M. Braun, *Phys. Rev.* **D52** (1995) 3929.
- [47] T. van Ritbergen, *Phys. Lett.* **B454** (1999) 353.
- [48] I.I. Bigi, M.A. Shifman, N.G. Uraltsev and A.I. Vainshtein, *Phys. Rev.* **D56** (1997) 4017.
- [49] A.A. Penin and A.A. Pivovarov, *Phys. Lett.* **B435** (1998) 413; *Nucl. Phys.* **B549** (1999) 217.
- [50] K. Melnikov and A. Yelkhovsky, *Phys. Rev.* **D59** (1999) 114009.
- [51] B.A. Kniehl and A. Penin, *Ultrasoft effects in heavy-quarkonium physics* [hep-ph/9907489].
- [52] B.A. Kniehl and A. Penin, *Order $\alpha_s^3 \ln^2(1/\alpha_s)$ corrections to heavy-quarkonium creation and annihilation* [hep-ph/9911414].
- [53] ECFA/DESY LC Physics Working Group (E. Accomando *et al.*), *Phys. Rep.* **299** (1998) 1.
- [54] I.I. Bigi *et al.*, *Phys. Lett.* **B181** (1986) 157.
- [55] V.S. Fadin and V.A. Khoze, *Pis'ma Zh. Eksp. Teor. Fiz.* **46**, 417 (1987) [*JETP Lett.* **46**, 525 (1987)]; *Yad. Fiz.* **48**, 487 (1988) [*Sov. J. Nucl. Phys.* **48**(2), 309 (1988)].
- [56] M.J. Strassler and M.E. Peskin, *Phys. Rev.* **D43** (1991) 1500.
- [57] W. Kwong, *Phys. Rev.* **D43** (1991) 1488; M. Jezabek, J.H. Kühn and T. Teubner, *Z. Phys.* **C56** (1992) 653; H. Murayama and Y. Sumino, *Phys. Rev.* **D47** (1993) 82; M. Jezabek and T. Teubner, *Z. Phys.* **C59** (1993) 669; Y. Sumino, K. Fujii, K. Hagiwara, H. Murayama and C.-K. Ng, *Phys. Rev.* **D47** (1993) 56; K. Fujii, T. Matsui and Y. Sumino, *Phys. Rev.* **D50** (1994) 4341; R. Harlander, M. Jezabek, J.H. Kühn and T. Teubner, *Phys. Lett.* **B346** (1995) 137; M. Jezabek *et al.*, *Phys. Rev.* **D58** (1998) 014006.

- [58] A.H. Hoang and T. Teubner, *Phys. Rev.* **D58** (1998) 114023; K. Melnikov and A. Yelkhovsky, *Nucl. Phys.* **B528** (1998) 59; O. Yakovlev, *Phys. Lett.* **B457** (1999) 170.
- [59] T. Nagano, A. Ota and Y. Sumino, *Phys. Rev.* **60** (1999) 114014.
- [60] A.A. Penin and A.A. Pivovarov, *Analytical results for $e^+e^- \rightarrow t\bar{t}$ and $\gamma\gamma \rightarrow t\bar{t}$ observables near the threshold up to the next-to-next-to-leading order of NRQCD* [hep-ph/9904278].
- [61] M. Peter and Y. Sumino, *Phys. Rev.* **D57** (1998) 6912.
- [62] K. Melnikov and O. Yakovlev, *Phys. Lett.* **B324** (1994) 217; V.S. Fadin, V.A. Khoze and A.D. Martin, *Phys. Rev.* **D49** (1994) 2247; W. Beenakker, F.A. Berends, A.P. Chapovsky, *Phys. Lett.* **B454** (1999) 129.
- [63] A.A. Penin and A.A. Pivovarov, *Nucl. Phys.* **B550** (1999) 375.
- [64] V.A. Novikov *et al.*, *Phys. Rev. Lett.* **38** (1977) 626; **38** (1977) 791 (E); *Phys. Rep.* **41** (1978) 1.
- [65] M.B. Voloshin and Yu.M. Zaitsev, *Usp. Fiz. Nauk.* **152** (1987) 361 [*Sov. Phys. Usp.* **30**(7) (1987) 553].
- [66] M.B. Voloshin, *Int. J. Mod. Phys.* **A10** (1995) 2865.
- [67] A.H. Hoang, *Phys. Rev.* **D59** (1999) 014039.
- [68] A.H. Hoang, *Heavy quark masses from the $Q\bar{Q}$ threshold and the epsilon expansion* [hep-ph/9909356].
- [69] M. Beneke, A. Signer and V.A. Smirnov, *A two-loop application of the threshold expansion: The bottom quark mass from b anti- b production* [hep-ph/9906476].
- [70] V. Giménez, L. Giusti, F. Rapuano and G. Martinelli, *NNLO unquenched calculation of the b quark mass* [hep-lat/9909138].